Results of a Transient Magnetotelluric Survey over a Buried Valley System in Southern Manitoba

David K. Goldak, M.Sc., P.Eng.

Abstract

Thunderstorm activity produces large amounts of electromagnetic energy which is trapped within the earth-ionosphere waveguide. The random sum of energy from activity on a near global scale produces a low-level quasi-continuous source field. Very large, or equivalently, relatively nearby lightning discharges produce *individual* transient events whose amplitude are significantly larger than that of the low-level background field. Therefore, the best possible signal-to-noise ratio is realized by recording exclusively sources of a transient nature. However, the transient events are strongly linearly polarized, the polarization diversity of which can affect the estimation of earth response curves.

It has been shown that an adaptive time domain averaging of the transient waveforms results in earth response curves whose bias converges to zero super-exponentially in stacked signal-to-noise ratio (Goldak et al., 2001). The efficacy of the algorithm is shown in the results of a transient audio-magnetotelluric (TAMT) survey conducted over a buried valley system in southern Manitoba, Canada. Twenty three sites at 200 m spacing were collected with the impedance tensor $\tilde{\mathbf{Z}}$ and the magnetic field tipper $\tilde{\mathbf{T}}$ estimated over the bandwidth 8 Hz - 32 kHz.

The results of the TAMT survey agree very well with those of a time domain electromagnetic (TEM) survey conducted by the Saskatchewan Research Council with a Geonics EM-47 over nearly the same profile.

Two dimensional OCCAM inversion of the TAMT data reveal the buried valley to be approximately 1 km wide, 70 m deep with a resistivity of approximately 12 $\Omega - m$, incised into Cretaceous sediments of approximately 4 $\Omega - m$ resistivity.

Contents

1 Introduction

The magnetotelluric (MT) method is a geophysical exploration technique in which the earth's electrical structure at depth may be determined from surface measurements of naturally occurring fluctuations in the earth's geomagnetic field, along with electric field fluctuations induced within the earth by the former.

The chief source of naturally occurring energy in the ELF/VLF[1] bandwidth is due to lightning discharges (Pierce, 1977. Volland, 1982). Thunderstorm activity on a near global scale produces a low level, quasi-continuous component, superimposed on which, are *individual* transients which arise from either relatively nearby and/or very large current-moment lightning discharges (Tzanis and Beamish, 1987. Jones and Kemp, 1971). Note that nearby is defined relative to global waveguide attenuation. For example, nearby at 100 Hz may be 6 Mm [2] whereas at 5 kHz, perhaps 1.5 Mm.

Both energy sources can be used to estimate earth response curves, but as shown in Figure 1, the best possible signal-to-noise ratio (SNR) is provided by the transient component.

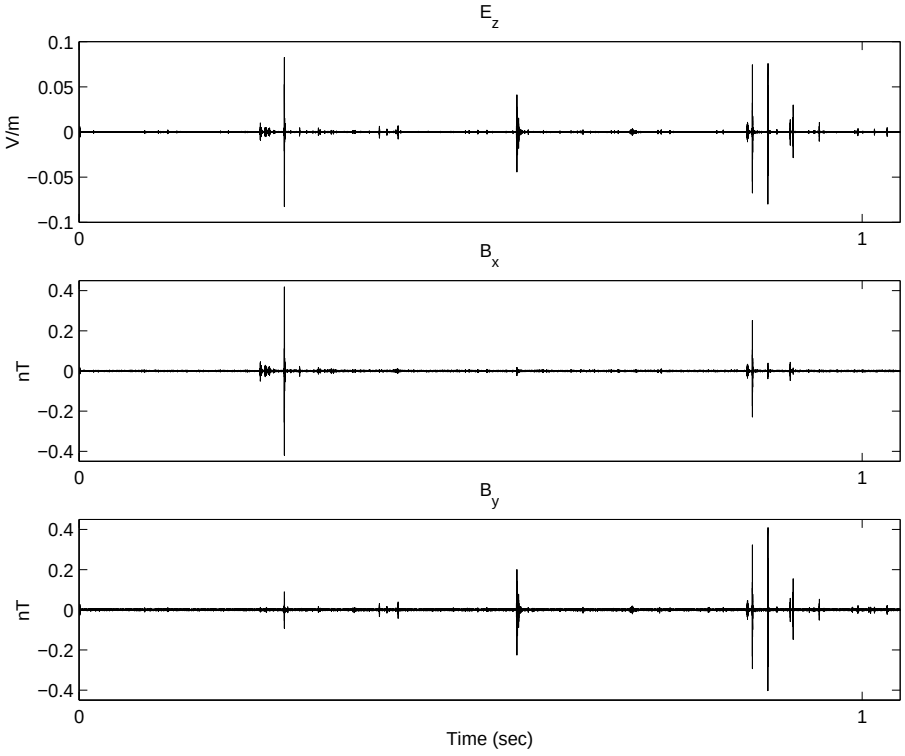

Figure 1: A typical VLF recording, Oct 18, 2001

Therefore, SFERIC, designed and constructed by EMpulse Geophysics Ltd., captures only transient energy in the 8 Hz - 32 kHz bandwidth. All parameter estimation is carried out with our Adaptive Polarization Stacking (APS) algorithm (Goldak et al., 2001), designed to work specifically with linearly polarized transient data.

In contrast with Remote-Reference (RR), our error analysis makes no assumptions about the statistical distribution of the noise or the circularity of the source field. We have further shown that the APS method has a higher order bias convergence than RR (Gamble et al., 1979) given typical polarization characteristics of transient data (Goldak et al., 2001).

[1] ELF: Extremely-Low Frequency, 3 Hz - 3 kHz; VLF: Very-Low Frequency, 3 kHz - 30 kHz

[2] 1 $Mm = 1000\ km$

2 Theory

The fundamental quantity of interest for MT surveys is the impedance tensor $\tilde{\mathbf{Z}}$ which is the transfer function between mutually orthogonal, horizontal components of magnetic and electric fields as defined in equation (1). Implicit in the definition of the impedance tensor is that we work in the frequency domain, with a right handed co-ordinate system defined as ^+x North, ^+y East and ^+z down.

$$\begin{bmatrix} \tilde{E}_x \\ \tilde{E}_y \end{bmatrix} = \begin{bmatrix} \tilde{Z}_{xx} & \tilde{Z}_{xy} \\ \tilde{Z}_{yx} & \tilde{Z}_{yy} \end{bmatrix} \cdot \begin{bmatrix} \tilde{H}_x \\ \tilde{H}_y \end{bmatrix} \tag{1}$$

or simply

$$\tilde{\mathbf{E}} = \tilde{\mathbf{Z}}\tilde{\mathbf{H}}.$$

Also of interest is the magnetic field tipper $\tilde{\mathbf{T}}$ as defined below in equation (2),

$$\tilde{H}_z = \tilde{T}_x\tilde{H}_x + \tilde{T}_y\tilde{H}_y. \tag{2}$$

The magnetic field tipper is sensitive to lateral changes in earth resistivity structure and is therefore very useful for locating discrete features and for assessing data dimensionality. Note that for a one-dimensional earth there exists no vertical magnetic field of secondary origin and thus $\tilde{\mathbf{T}}$ vanishes.

However, if we consider estimation of $\tilde{\mathbf{Z}}$ only, the regression problem is typically solved by minimizing the sum square error of the residual on the electric or magnetic field channels. This gives rise to the familiar least squares solution of $\tilde{\mathbf{Z}}$ which involves the estimation of auto and cross-spectral densities.

Consider another approach, note that since we have four complex unknowns and only two equations, we need at least two independent measurements of equation (1) to solve for $\tilde{\mathbf{Z}}$. If we consider this simplest case, we have,

$$\begin{aligned} \tilde{E}_{xi} &= \tilde{Z}_{xx}\tilde{H}_{xi} + \tilde{Z}_{xy}\tilde{H}_{yi} \\ \tilde{E}_{yi} &= \tilde{Z}_{yx}\tilde{H}_{xi} + \tilde{Z}_{yy}\tilde{H}_{yi} \\ i &= 1, 2. \end{aligned} \tag{3}$$

Solving this pair of 2 x 2 linear systems yields the two-point formulas for $\tilde{\mathbf{Z}}$. The modifier two-point is used as although these are complex variables, the solution is analogous to passing a plane through the origin and two other points.

Until now, statistical analysis of the bias in estimates of $\tilde{\mathbf{Z}}$ has been done for conventional least-squares (Sims et al., 1971) and remote-reference (RR) (Gamble et al., 1979) solutions, but not for the two-point solution. Although it was claimed that RR is "unbiased" (Gamble et al., 1979), this is valid only in the limit of infinitely many independent measurements. Practically then, the solutions of $\tilde{\mathbf{Z}}$ just mentioned in fact display a finite convergence of bias as SNR becomes large. However, for RR and APS, there is also a bias convergence to some arbitrarily small level at fixed SNR, simply as the number of measurements N becomes large.

The LS solution has a bias that converges as a function of SNR only, as SNR^{-2} approximately. By contrast, the bias in the two-point formula is due only to nonlinearity in the complex quotient. Its bias is of infinitely smaller order, namely $exp(-\frac{1}{2}(ISNR\sin(\alpha))^2)$, where α is the angle between the stacked events ($0 \leq \alpha \leq 90^\circ$) and $ISNR$ is the improved SNR gained by stacking the time domain waveforms.

By averaging the time domain waveforms the noise would ideally grow only as $\sqrt{N}$ and the signal as N, giving an overall $\sqrt{N}$ enhancement of SNR. However, the shape of the transient waveforms can be quite variable so in practice, we typically achieve an SNR enhancement on the order of $0.6 - 0.7 \times \sqrt{N}$ (Figure 2).

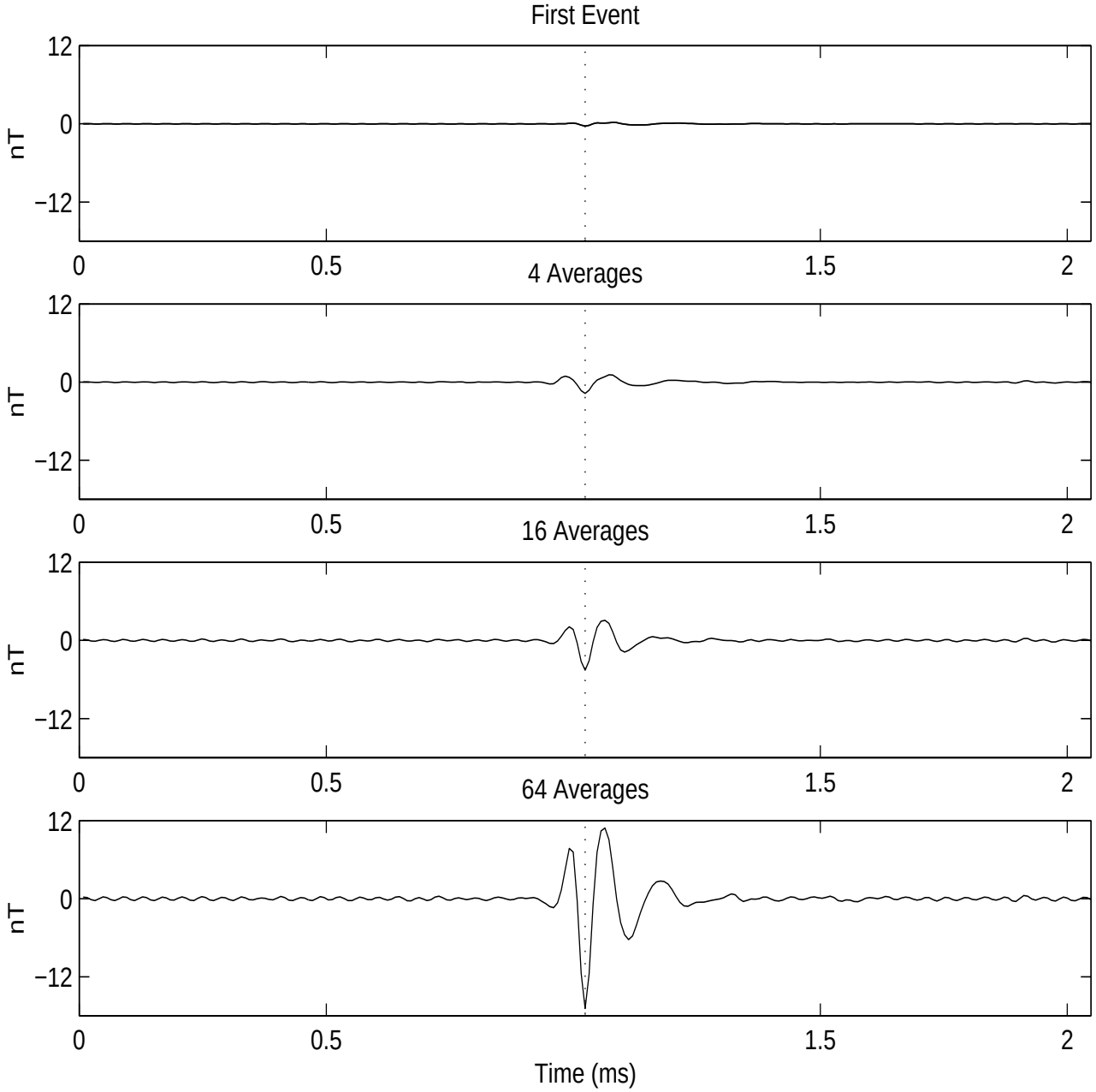

Figure 2: SNR enhancement

However, the polarization diversity of received transients may be such that α is much less than the optimal 90° (Figure 3), but even for $\alpha = 30°$, the reduction factor of $\sin(\alpha) = 0.5$ is quickly offset by the improvement in SNR. At only moderate ISNR and angle α, the stacking bias can already be less than $10^{-7}|\tilde{\mathbf{Z}}|$ and hence negligible in single precision (Goldak et al., 2001).

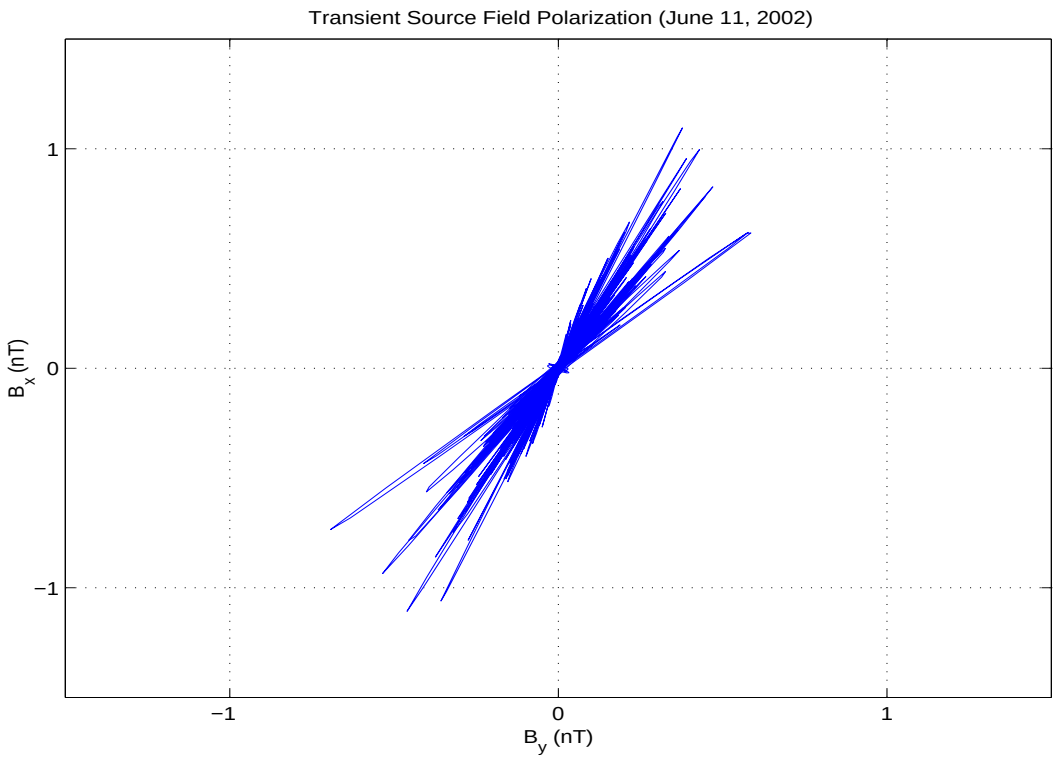

Figure 3: Hodogram of horizontal magnetic flux density

Furthermore, for RR error analysis to be valid, we require not only infinitely many independent measurements but also a circularly polarized source field (Gamble et al., 1979). As shown in Figure 3, the polarization diversity of transient data is often non-uniform with incoming energy confined to one quadrant only. The approximation of a circularly polarized source field is poorly realized in many cases.

Conversely, our APS error analysis makes no assumptions about the statistical distribution of the noise or the polarization diversity of the source field. Our error bars are derived through Monte-Carlo simulation where the residual between predicted and measured data controls how much the measured data gets perturbed. This is done many times over to observe a noisy family of curves from which 95 percent confidence limits are found.

Note that for a good inversion to be conducted, well estimated error bars are arguably as important as the curves themselves.

3 Results

In 1995 the Saskatchewan Research Council (SRC) was contracted by the Geological Survey of Canada (GSC) to conduct time domain electromagnetic soundings in locations deemed prospective for buried valley type aquifers.

The SRC used an EM-47 with 40 m x 40 m single turn square loop typically carrying on the order of 2 Amps current. Two sweeps were employed with 75 and 300 Hz repetition rates, with centrally located, in loop measurements only.

This study is concerned with one profile only, located in southern Manitoba approximately twenty kilometres south-east of the town of Melita.

Unfortunately, this line was stationed in a ditch very close to a medium sized three-phase powerline. Therefore, the late time gates of the 75 Hz TEM data are extremely noisy and thus provided

very little additional depth information. The 300 Hz TEM data are reasonable quality except for the two or three latest time gates.

A transient audio-magnetotelluric (TAMT) survey was conducted over the same buried valley system in early November, 2001, although displaced 500 m to the north of the powerline so as to lessen cultural noise effects.

Note that for a 1D isotropic earth, the impedance tensor $\tilde{\mathbf{Z}}$ takes on a very simple form, namely,

$$\tilde{Z}_{xy} = \frac{\tilde{E}_x}{\tilde{H}_y} = -\tilde{Z}_{yx} = -\frac{\tilde{E}_y}{\tilde{H}_x}, \ \tilde{Z}_{xx} = \tilde{Z}_{yy} = 0. \tag{4}$$

We see that the modulus of the two non-zero components of $\tilde{\mathbf{Z}}$ are equal and the argument of the two components are shifted by 180 degrees [3]. Of course in the 1D anisotropic case the modulus of $\tilde{\mathbf{Z}}$ is no longer single valued, the only way to distinguish a 1D anisotropic earth from a 2D earth is by measurement of $\tilde{\mathbf{T}}$.

Although one is mainly concerned with the estimation of $\tilde{\mathbf{Z}}$, for display purposes we usually present the apparent resistivity, denoted ρ (scaled modulus of $\tilde{\mathbf{Z}}$), and phase ϕ. Similarily, for $\tilde{\mathbf{T}}$, the real and imaginary parts are plotted separately. The apparent resistivity of all four components of $\tilde{\mathbf{Z}}$ are shown in Figure 4.

We see that $\tilde{\rho}_{xy} \approx \tilde{\rho}_{yx}$ and that $\tilde{\rho}_{xx}$ and $\tilde{\rho}_{yy}$ are zero to within the noise level of the data, thus satisfying the conditions for a 1D isotropic earth.

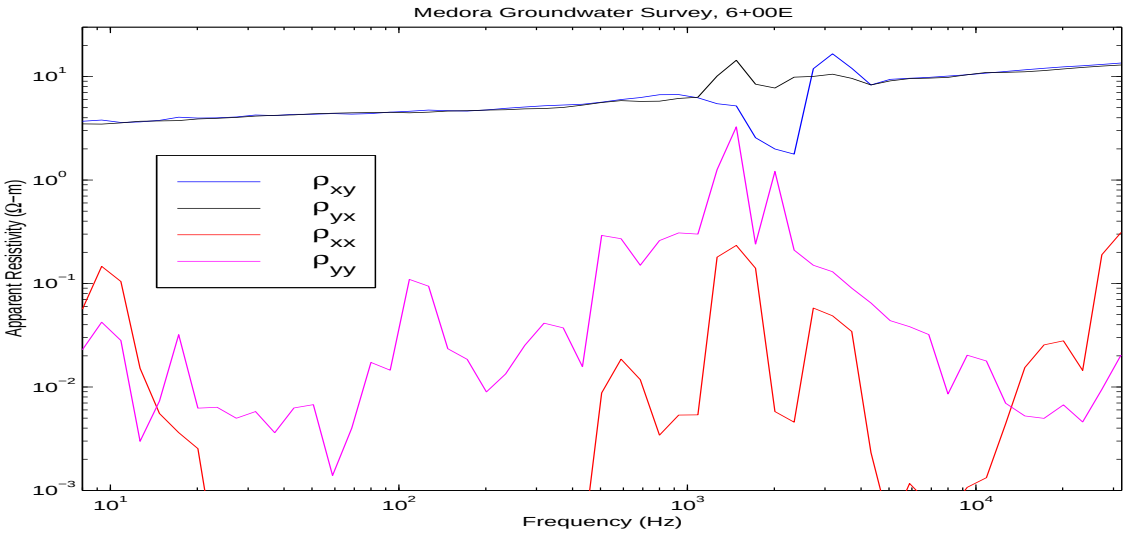

Figure 4: One-Dimensional Isotropic Earth

The ragged character of the earth response curves in the range 1 to 4 kHz result from the intense earth-ionosphere waveguide attenuation in this frequency range, the so called AMT "dead-band". It is only when thunderstorm activity is in the range 500-2000 km that the curves may pass smoothly through the dead-band. However, this recording was made in early November when the closest sources of transient excitation were in the Gulf of Mexico and the North Atlantic, both in excess of 3000 km great circle distance.

For presentation purposes, we interpolate linearly through the dead band in cases when it is needed. This is done with the knowledge that the earth response curves are the result of a convolutional process and are therefore slowly varying functions of frequency (Figure 5). However, data errors are not interpolated. Thus for the final inversion, editing of the curves themselves has little effect on the final inverted model as the dead-band error bars will be very large if the curves require interpolation.

[3] Although it is often seen that $\tilde{\phi}_{yx}$ is shifted to the first quadrant by addition of 180 degrees.

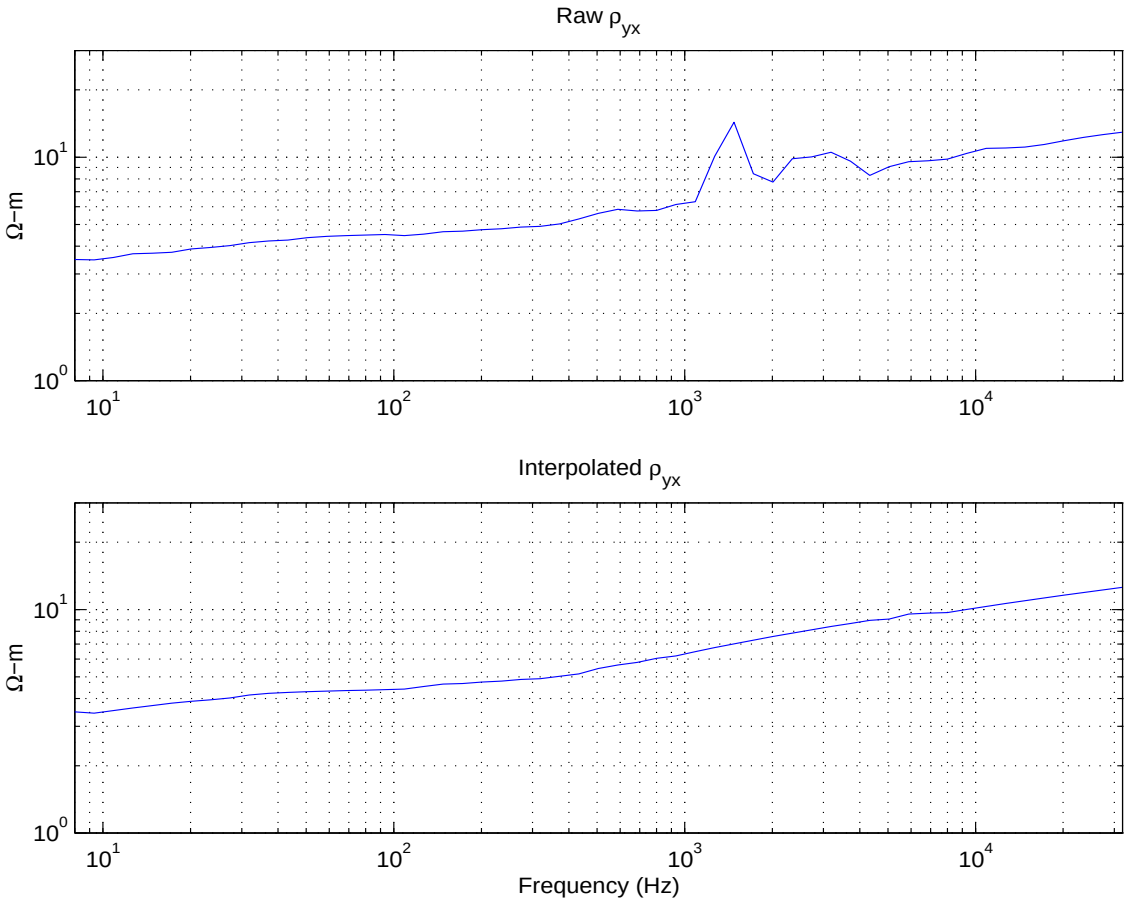

Figure 5: Raw and Interpolated $\tilde{\rho}_{yx}$

Shown on the following three pages are the interpolated earth response curves. Evidence of the paleochannel is clearly seen on $\tilde{\rho}_{xy}$, $\tilde{\rho}_{yx}$ and $\tilde{\phi}_{yx}$.

Note that the data are for the most part extremely 1D, it is only near the edges of the paleochannel that we see some 2D effects. This is corroborated in the plot of the tipper data. The tipper is very small except at two locations which approximately define the edges of the paleochannel, although not strictly so as the tipper is sensitive to features laterally displaced from the measurement site.

Note that the tipper anomaly is quite small, as a percentage of the horizontal field, approximately ten percent on the real component and five percent on the imaginary component.

Melita Groundwater Survey

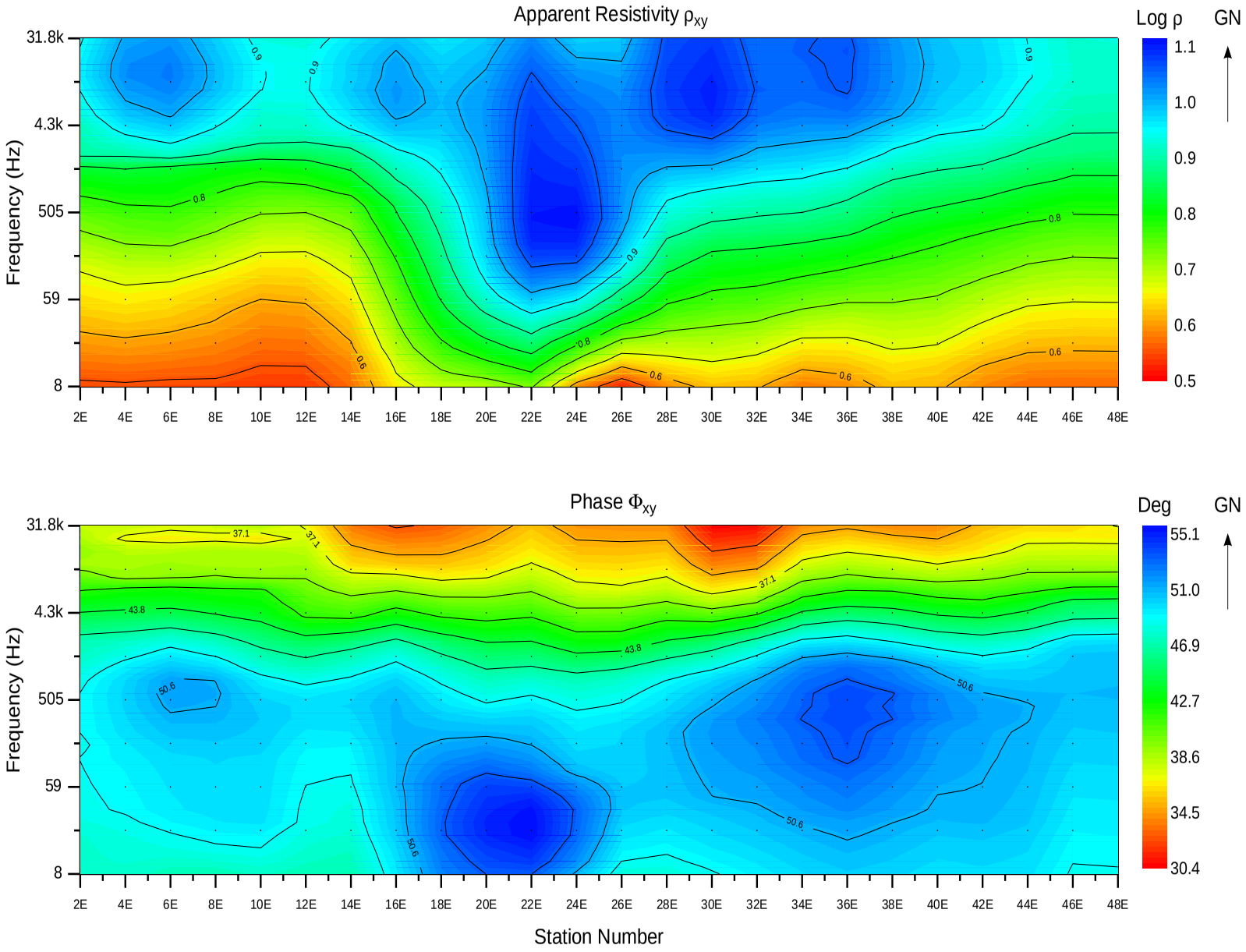

Melita Groundwater Survey

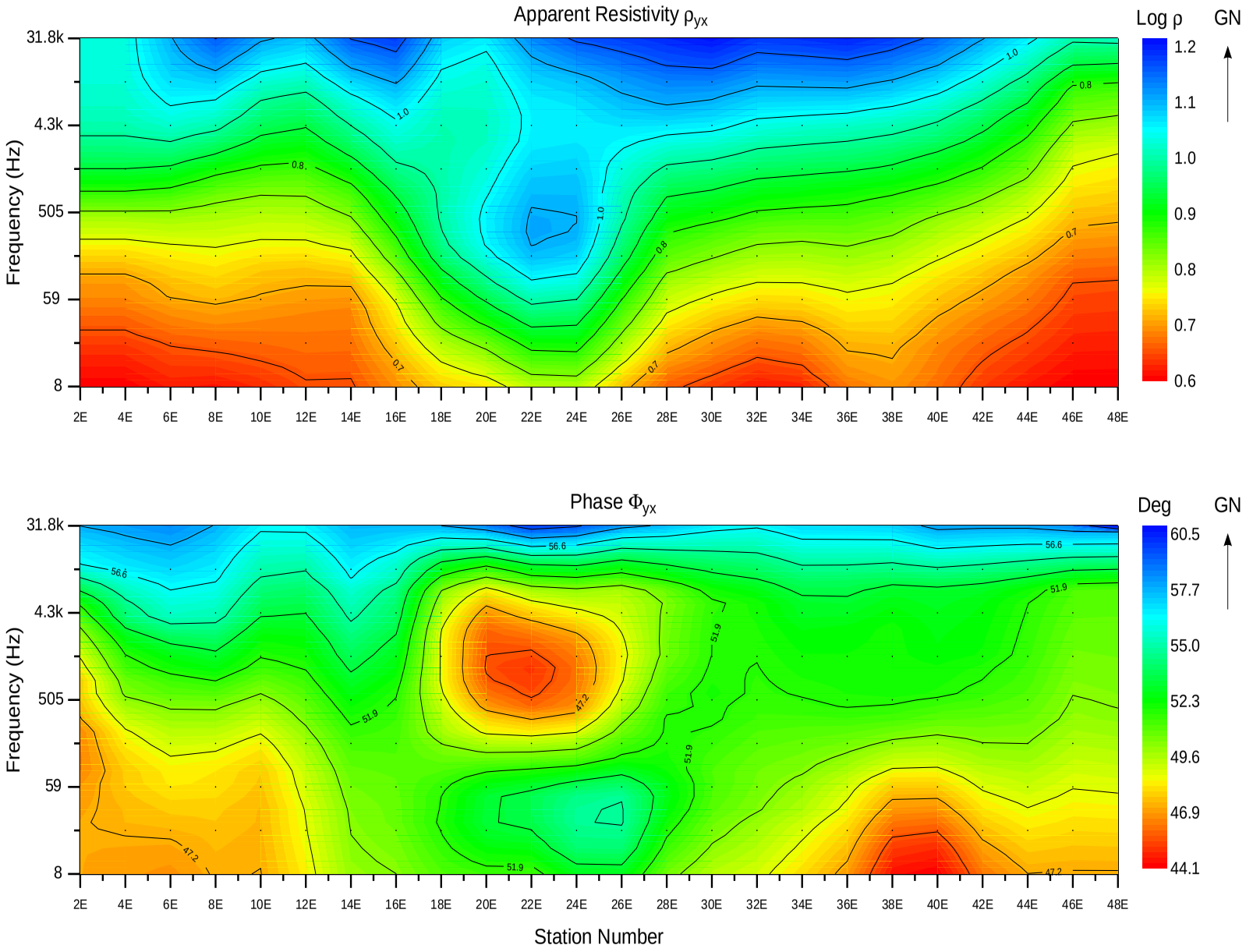

∞

Melita Groundwater Survey

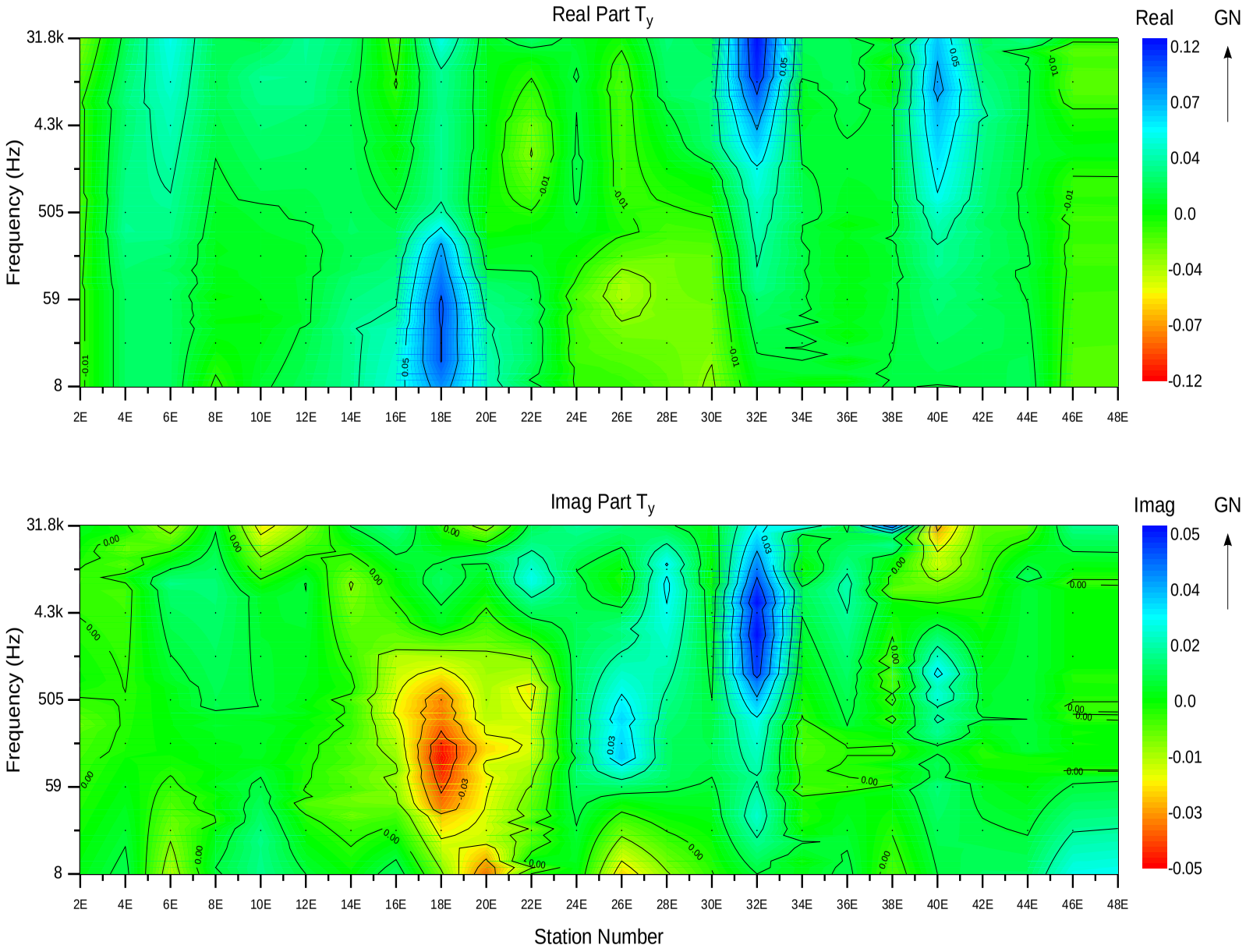

One-dimensional interpretation of the TAMT and EM-47 data is shown below. Note that the TAMT data have not been inverted in the truest sense but rather simply transformed. The Bostick transform (Bostick, 1977) is an approximate 1D inversion method for MT data that approximates a first-order image solution for the time-domain EM case (Nekut, 1982). This results in a smoothly varying resistivity profile as a function of (pseudo) depth which may not be the best approximation if the earth structure is truly layered as it appears to be for this data-set.

On the other hand, the EM-47 data have been inverted with a layered earth, iterative L.S. fitting process. However, note that neither of these 1D interpretive methods incorporate data errors in their analysis. Also, the Bostick transformed results of the TAMT data extend well past 275 m (pseudo) depth, for comparison with the EM-47 data though a reduced depth scale was used.

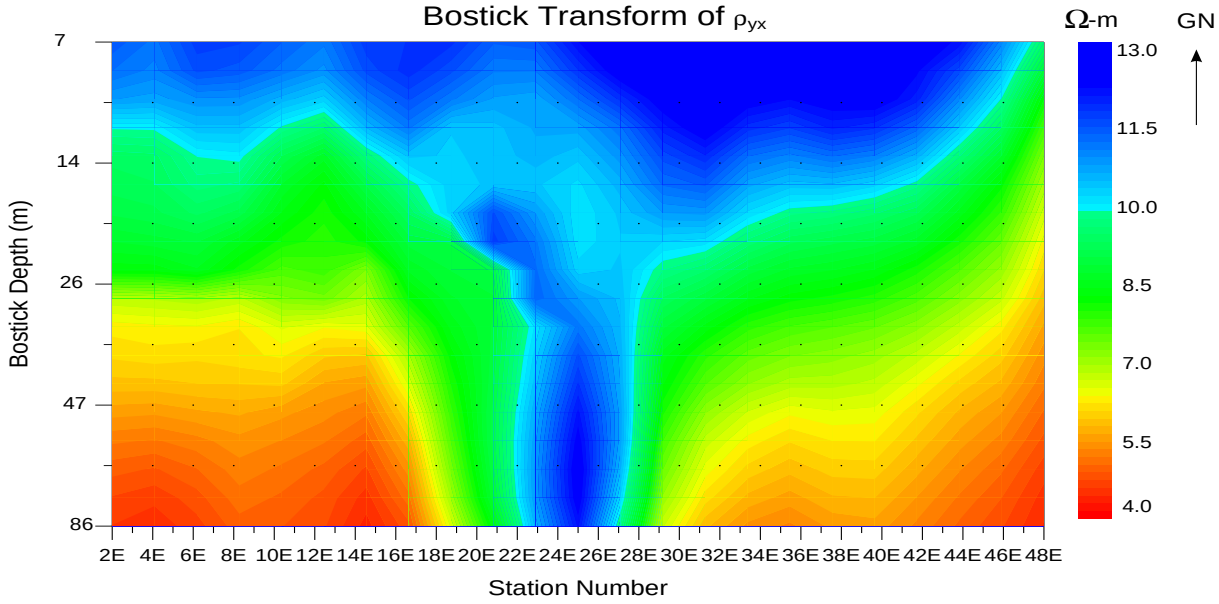

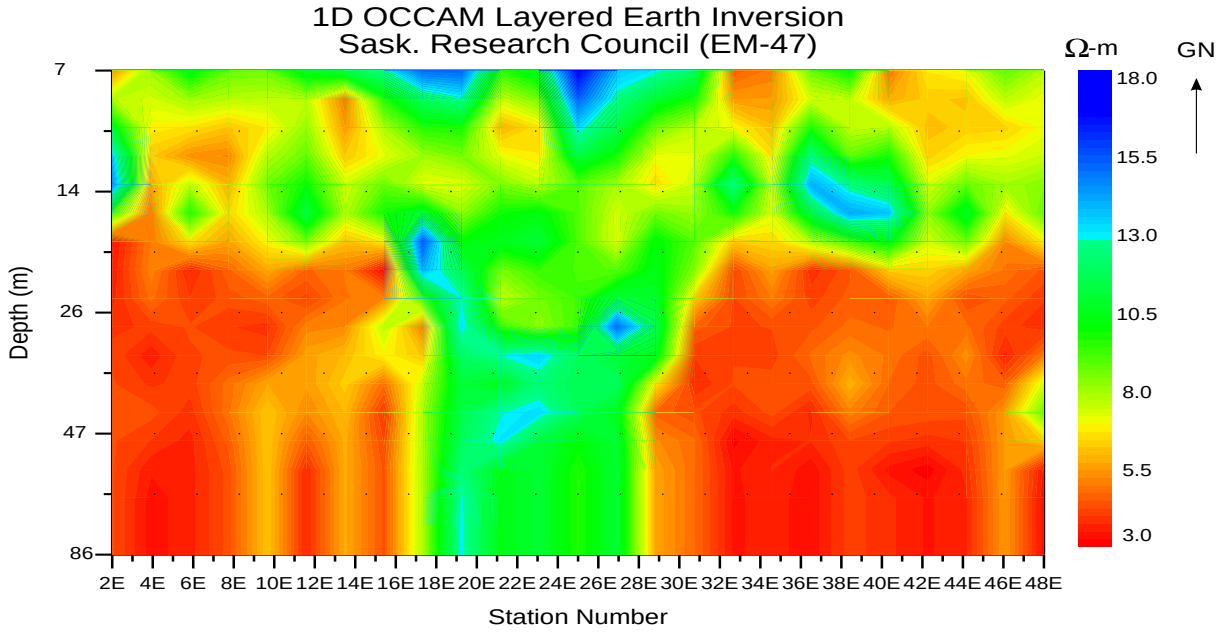

We see that the TAMT data seems to be mapping the resistive drift in a superior fashion while the EM-47 data seems to be better mapping the depth to the marine Cretaceous shales. However, note the different resistivity scales in the two plots.

Shown lastly is the 2D OCCAM inversion (deGroot-Hedlin et al., 1990) of the TAMT data. The 2D inversion is the most rigorous as the data around the edges of the paleochannel are 2D and data errors are fully utilized.

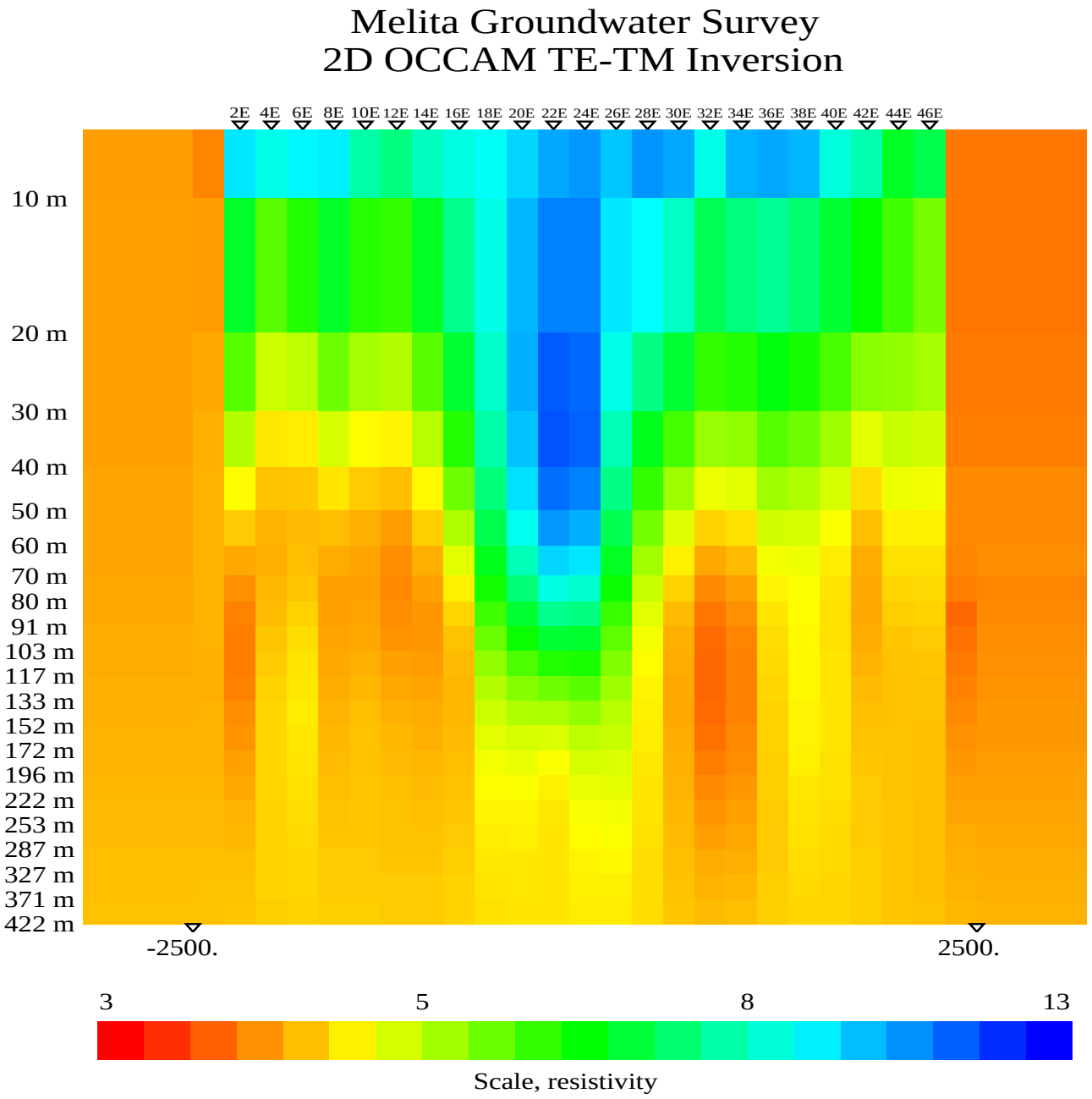

We see the edges of the paleochannel at approximately 18E and 26E, the resistivity of the drift is $\approx 12\ \Omega - m$ while that of the Cretaceous marine shales, $\approx 4\ \Omega - m$. The depth to the bottom of the paleochannel is approximately 70 m at stations 22E and 24E. Immediately to the east of the paleochannel the drift is roughly 20 m thick, while 10 m otherwise.

This generally agrees with the study of Betcher (1983) who indicates that 20 m of drift over Cretaceous "bedrock" is typical while the largest amount of drift observed within the channel was 82 m.

The depth range 20-40 m approximately covers the so called AMT dead-band where data errors are largest. Based on the EM-47 data, the Cretaceous shales should extend up to 20 m depth or so on the 2D TAMT inversion. However, due to the larger data errors in this frequency range the inversion code is not required to put any structure here, it is not until about 40 m depth when the error bars tighten up that we clearly image the marine shales.

4 Conclusions

The largest naturally occurring signals in the ELF/VLF bandwidth are transients. In order to record transients most efficiently, a time localized recording technique is desired. In so doing, the best possible SNR in the raw data is obtained.

By performing an adaptive time domain averaging of the transient waveforms we obtain essentially unbiased estimates of the impedance tensor or magnetic field tipper while using only four or three channels of data respectively.

The effectiveness of the algorithm has been displayed with real data in the mapping of a buried valley system in southern Manitoba. Further verification is provided by the good agreement with EM-47 data collected by the Saskatchewan Research Council on nearly the same profile.

In agreement with Betcher (1983), we find the paleochannel to be roughly 1 km wide, 70 m deep with a resistivity of $\approx 12\ \Omega - m$, incised into Cretaceous shales of $\approx 4\ \Omega - m$ resistivity.

5 Acknowledgements

The assistance of the primary authors wife, Sheila Goldak, during the field work of this project was greatly appreciated. We would also like to thank the Saskatchewan Research Council, Mark Simpson and Dennis Zlipko in particular, for releasing their data and for their abundant assistance in choosing a survey location. We would also like to thank Cameco Corporation for the use of their computing facilities in the inversion of the EM-47 data, the assistance of Lawrence Bzdel and Garnet Wood was much appreciated. Lastly, Dr. Michael Leppin of Cameco Corporation is thanked for the many interesting discussions concerning multi-dimensional electromagnetic inversion.

References

[1] Betcher, R.N., 1983, Groundwater availability map series, Virden area (62F), Manitoba Natural Resources, Water Resources, Figure 3, 1:250,000 scale map.

[2] Bostick, F.X., 1977, Workshop on electrical methods in geothermal exploration, U.S. Geological Survey contract number 14-08-001-G-359.

[3] deGroot-Hedlin, C and Constable, S., 1990, Occam's inversion to generate smooth, two-dimensional models from magentotelluric data, Geophysics, **55**, 1613-1624.

[4] Gamble, T.D., Goubau, W.M. and Clarke, J., 1979, Error analysis for remote reference magnetotellurics, Geophysics,**44**, 959-968.

[5] Goldak, D.K. and Goldak, S., 2001, Transient Magnetotellurics with Adaptive Polarization Stacking, presented at SEG International Exposition and 71'st Annual Meeting, 2001, San Antonio.

[6] Jones, D.L. and Kemp, D.T., 1971, The nature and average magnitude of the sources of transient excitation of Schumann resonances, Journal of Atmospheric and Terrestrial Physics, **33**, 557-566.

[7] Nekut, A.G., 1982, Direct inversion of time-domain electromagnetic data, Geophysics,**52**, 1431-1435.

[8] Pierce, E.T., 1977, Atmospherics and radio noise, in Golde, R.H., ed., Lightning,**1**, Academic Press.

[9] Sims, W.E., Bostick, F.X. and Smith, H.W., 1971, The estimation of magnetotelluric impedance tensor elements from measured data, Geophysics, **36**, 938-942.

[10] Tzanis, A. and Beamish, D., 1987, Audiomagnetotelluric sounding using the Schumann resonances, Journal of Geophysics,**61**, 97-109.

[11] Volland, H., 1982, Low fregrency radio noise, in Volland, H., ed., CRC Handbook of atmospherics,**1**, CRC Press Inc.